



**HAL**  
open science

## Design, Synthesis, and Evaluation of Neomycin-Imidazole Conjugates for RNA Cleavage

Céline Martin, Maurinne Bonnet, Nadia Patino, Stéphane Azoulay, Audrey Di  
Giorgio, Maria Duca

► **To cite this version:**

Céline Martin, Maurinne Bonnet, Nadia Patino, Stéphane Azoulay, Audrey Di Giorgio, et al.. Design, Synthesis, and Evaluation of Neomycin-Imidazole Conjugates for RNA Cleavage. *ChemPlusChem*, 2022, 87 (11), 10.1002/cplu.202200250 . hal-03852428

**HAL Id: hal-03852428**

**<https://hal.science/hal-03852428>**

Submitted on 15 Nov 2022

**HAL** is a multi-disciplinary open access archive for the deposit and dissemination of scientific research documents, whether they are published or not. The documents may come from teaching and research institutions in France or abroad, or from public or private research centers.

L'archive ouverte pluridisciplinaire **HAL**, est destinée au dépôt et à la diffusion de documents scientifiques de niveau recherche, publiés ou non, émanant des établissements d'enseignement et de recherche français ou étrangers, des laboratoires publics ou privés.

## **Design, synthesis and evaluation of neomycin-imidazole conjugates for RNA cleavage**

Dr. Céline Martin,<sup>†</sup> Maurinne Bonnet,<sup>†</sup> Prof. Nadia Patino, Prof. Stéphane Azoulay, Dr. Audrey Di Giorgio, Dr. Maria Duca\*<sup>[a]</sup>

<sup>[a]</sup> Université Côte d'Azur, CNRS, Institute of Chemistry of Nice (ICN), Nice, France

<sup>†</sup> These authors contributed equally to this work

**Keywords:** RNA targeting, RNA cleavage, neomycin, conjugate, inhibition

## **Abstract**

Targeting RNA with synthetic small molecules attracted much interest during recent years as a particularly promising therapeutic approach in a large number of pathologies spanning from genetic disorders, cancers as well as bacterial and viral infections. In this work, we took advantage of a known RNA binder, neomycin, to prepare neomycin-imidazole conjugates mimicking the active site of ribonuclease enzymes able to induce a site-specific cleavage of HIV-1 TAR RNA in physiological conditions. These new conjugates were prepared using a straightforward synthetic methodology and were studied for their ability to bind the target, inhibit Tat/TAR interaction and induce selective cleavage using fluorescence-based assays and molecular docking. We found compounds with nanomolar affinity, promising cleavage activity and the ability to inhibit Tat/TAR interaction with submicromolar  $IC_{50}$ s.

## Introduction

The search for selective binders of biologically relevant RNAs is a growing field of medicinal chemistry and chemical biology.<sup>[1]</sup> Indeed, even if rational methodologies for the design of such ligands are not in an advanced stage as for protein targeting, small molecules able to specifically bind and inhibit RNA functions hold the promise for important developments for the study of RNAs biological functions as well as for the treatment of incurable diseases where these RNAs are involved.<sup>[2]</sup> Targeting of coding and non-coding RNAs has been successfully achieved using oligonucleotides that are able to recognize in a sequence-specific manner the RNA target thanks to base complementarity.<sup>[3]</sup> However, the application of these tools *in vivo* and in clinic remains limited due to a number of pharmacological limitations. For this reason, an approach based on the use of small molecules has been developed to target RNAs and represents a promising route to interfere with RNA biological and pathological functions.<sup>[4]</sup>

Various types of small molecules have been developed for the specific targeting of viral, bacterial and oncogenic RNAs. For example, the targeting of procaryotic ribosomal RNAs succeeded thanks to various classes of antibiotics such as aminoglycosides, tetracyclines, macrolides and many others.<sup>[5]</sup> More recently, the identification of Risdiplam as a modulator of pre-mRNA splicing in spinal muscular atrophy (SMA) paved the way for new therapies for this rare and deadly genetic disease, but also for other unmet medical needs.<sup>[6]</sup> Major results in the targeting of RNA using small molecules have been obtained also against oncogenic microRNAs using a methodology called InfoRNA that allows for the combination of advanced screening and bioinformatic tools leading to the discovery of very specific and efficient inhibitors of the biogenesis of oncogenic miRNAs *in vitro* and *in vivo*.<sup>[7]</sup> Various methodologies have thus been developed during the last years that led to the identification of promising compounds against relevant RNA targets.<sup>[1, 4]</sup>

While most RNA binders act by establishing a dynamic complex with their target, compounds able to bind and also cleave the target have been reported.<sup>[8]</sup> First of all, RNA ligands, such as small molecules peptides and oligonucleotides, have been coupled to histidine and imidazole residues to mimic the RNases active site that contains two histidine residues responsible for RNA cleavage.<sup>[9]</sup> Furthermore, compounds known to selectively bind a particular RNA target have been coupled to bleomycin.<sup>[10]</sup> This latter is an anticancer natural compound able to cleave DNA and RNA *via* the production of radical species that induce unspecific cleavage. Finally, an innovative strategy allowing for the *in vitro* and *in vivo* degradation of RNA targets has been developed similarly to PROTAC and called RIBOTAC.<sup>[11]</sup> In this approach, the RNA ligand is coupled to an RNase recruiting compound and the resulting conjugate is not only able to selectively bind to the desired target but also to induce the intracellular degradation of the target by RNases.

During recent years, we have developed the design of multifunctional ligands based on the conjugation of various known RNA binding motifs bringing both affinity and selectivity for the target.<sup>[12]</sup> This led

us for example to the preparation of conjugates of neomycin, artificial nucleobases and amino acids. While neomycin belongs to the aminoglycoside class of antibiotics able to bind many different types of RNA targets, artificial nucleobases are able to selectively interact with RNA base pairs. Concerning amino acids, they constitute proteins and peptides that are natural RNA binders. Some of the synthesized conjugates have shown promising results for the inhibition of oncogenic microRNAs production, *in vitro* and in cancer cells.<sup>[12d-f]</sup> These results demonstrated that even if aminoglycosides have been discovered many decades ago and, as mentioned above, they lack specificity for a particular RNA target, they still represent a source of inspiration for the preparation of new RNA ligands whose affinity and selectivity can be greatly improved upon chemical modification.<sup>[13]</sup> Concomitantly, we also pursued screening studies to search for new RNA binders with successful results both in the targeting of oncogenic microRNAs and viral RNAs.<sup>[14]</sup>

In this work, we decided to take advantage of the RNA binding properties of neomycin to explore its RNA cleavage ability upon conjugation with imidazole-containing compounds (Figure 1A). More specifically, we studied the effect of histidine conjugation to neomycin on the TAR RNA fragment that represents an ideal model as well as an interesting biological target. We demonstrate that the conjugation of histidine amino acid to neomycin improves affinity as compared to neomycin itself, and moreover induces selective RNA cleavage in physiological conditions and greatly increases the activity of inhibition of TAR interaction with its intracellular partners such as the Tat peptide.

## Results and Discussion

**Design and synthesis of new neomycin conjugates.** Neomycin belongs to the class of aminoglycoside antibiotics that are known to bind to procaryotic ribosomal RNA and impair protein synthesis.<sup>[15]</sup> Despite this precise mechanism of action, neomycin is also known as an efficient binder for other kinds of biologically relevant RNAs such as the HIV-1 TAR RNA.<sup>[16]</sup> This latter is a 59-nucleotide RNA fragment able to form a highly conserved stem-loop structure as illustrated in Figure 1B. TAR RNA plays a key role in viral replication because its interaction with the Tat protein allows for the formation of a complex involving cellular cofactors such as cyclin T1 and its cognate kinase CDK9, which thus stimulates efficient transcription from the retroviral promoter (LTR). The binding site for neomycin on TAR was identified using ribonuclease protection experiments and is located in the stem immediately below the three-nucleotide bulge that serves as the primary identity element for Tat.<sup>[16]</sup> The interaction between neomycin and TAR RNA was thus chosen as an ideal model to test how the conjugation of histidine residues on neomycin could induce not only a more efficient binding to RNA but also one or more cleavage sites on the target sequence. Indeed, it has been largely demonstrated in the past,<sup>[9,10]</sup> that introduction of histidine or imidazole residues on RNA binding agents could mimic the active site of RNase enzymes where histidine residues are present in the cleavage site and act in their protonated and unprotonated form at pH 7 and in the presence of divalent cations, such as Mg<sup>2+</sup>, to induce phosphodiester cleavage. We thus decided to design new conjugates of neomycin and histidine using

different kind of linkers. First of all, we chose to conjugate histidine amino acid using the same linker we employed in the past that showed successful results in terms of binding and selectivity and containing a triazole scaffold.<sup>[12d, 17]</sup> As demonstrated in our previous works, the triazole moiety can participate efficiently to RNA binding and allows for a straightforward synthesis thanks to the use of the copper-catalyzed 1,3-dipolar cycloaddition. To appreciate the involvement of this kind of linker in the interaction, we prepared the analog containing an amido linker between histidine and neomycin. This asks for the addition of a synthetic step, but the amide linker could also participate to the interaction. Finally, we prepared a third analog where a histidine residue lacking the  $\alpha$ -NH<sub>2</sub> group was conjugated using a triazole linker to evaluate the importance of this amino group in the interaction and, potentially, in the cleavage induced by the compound.

The synthesis of the designed conjugates first required the preparation of a derivative of neomycin bearing Boc protecting groups on the six amines and an azido group in position 5'' (Compound **Neo-N<sub>3</sub>**, Scheme 1) using a previously reported procedure.<sup>[12e]</sup> For the preparation of the conjugate containing histidine linked to neomycin through a triazole linker, a 1,3-dipolar cycloaddition was performed on **NeoN<sub>3</sub>** in the presence of *N*-Boc-L-His(Boc)-propargylamide (compound **8**, see supporting information for experimental details), CuI and DIPEA in CH<sub>3</sub>CN leading to fully Boc-protected derivative **1** in 96% yield. In a similar way, we prepared the conjugate containing the analog of histidine lacking the  $\alpha$ -NH<sub>2</sub> by performing the 1,3-dipolar cycloaddition in the presence of *N*-2-propyn-1-yl-1*H*-imidazole-5-acetamide (compound **10**, see supporting information for experimental details) CuI and DIPEA in CH<sub>3</sub>CN. This allowed us to obtain compound **2** in 63% yield. Following deprotection of **1** and **2** in the presence of TFA in CH<sub>2</sub>Cl<sub>2</sub> led to desired compounds **3** and **4** in 78% and 76% yields, respectively. Finally, the conjugate containing histidine linked to neomycin through an amide linker was synthesized after the initial reduction of NeoN<sub>3</sub> to its amino derivative **5** (see supporting information for experimental details) in the presence of H<sub>2</sub> and Pd/C in ethanol. The desired compound was obtained in 72% yield. The following coupling with *N*-Boc-L-His(Boc)-OH in the presence of HOSu and EDC in a CH<sub>2</sub>Cl<sub>2</sub>/DMF 1:1 solution led to conjugate **6** in 71% yield. Final cleavage of Boc groups by TFA in CH<sub>2</sub>Cl<sub>2</sub> led to compound **7** in 59% yield. All compounds were obtained with purities over 98% and were fully characterized by NMR and HRMS.

**Interaction of compounds 3, 4 and 7 with TAR RNA.** As mentioned above, we chose TAR RNA as a promising target for the development of new RNA ligands and as a model to explore the possibility to induce RNA cleavage with the synthesized compounds. First of all, we studied the affinity of the synthesized conjugates **3**, **4** and **7** for a 27-mer TAR RNA sequence. To this aim, we employed a well-known fluorescence-based assay where the RNA is labeled at 5'-end with a fluorophore (Alexa488<sup>TM</sup>). Binding of ligands on the RNA sequence affects the environment of the fluorophore thus changing its fluorescence emission and allowing for the measurement of dissociation constants ( $K_D$ ). As illustrated in Table 1 (see also Figure S1 in the Supporting Information), the three synthesized compounds were compared to neomycin, histidine amino acid, imidazole and finally to a commercial conjugate of

histidine and naphthalene (L-Histidine  $\beta$ -naphthylamide) known to be a non-specific intercalating agent. We observed that while neomycin has a  $K_D$  of  $1.74 \pm 0.16 \mu\text{M}$  in the employed conditions, compound **3** containing histidine conjugated *via* a triazole linker shows a much better affinity with a  $K_D$  of  $84 \text{ nM}$  ( $0.084 \pm 0.0015 \mu\text{M}$ ), more than 20 times lower than the one of neomycin itself. This shows that the simple addition of a histidine amino acid can greatly improve RNA binding. However, the nature of the linker between neomycin and the amino acid also plays a role in the interaction since the replacement of the triazole moiety (compound **3**) by an amide bond (compound **7**) leads to a slight loss of affinity ( $K_D$  of  $0.333 \pm 0.14 \mu\text{M}$ ). In addition, it can be noted that the presence of the  $\alpha$ -NH<sub>2</sub> on histidine seems to directly impact the affinity for TAR since its removal as in compound **4**, induces an increase in the  $K_D$  to  $1.38 \pm 0.17 \mu\text{M}$  that is similar to the one of neomycin. Finally, histidine and imidazole alone do not show any RNA binding in the employed range of concentration and L-histidine  $\beta$ -naphthylamide showed a  $K_D$  of  $13.6 \mu\text{M}$  which is 8 times higher than the one of neomycin and more than 150 times higher than the best ligand **3**. These data suggest that neomycin conjugation with a histidine residue using a suitable linker can greatly increase the affinity for a stem-loop structured RNA as TAR.

**RNA cleavage activity of the synthesized compounds.** As described above, compounds **3**, **4** and **7** were designed on the basis that histidine and imidazole moieties could induce cleavage when conjugated to various kinds of RNA ligands. Surprisingly, imidazole-containing moieties have never been conjugated to neomycin that is a well-known RNA binder able to interact with various RNA structures thanks to its aminoglycoside positively charged chemical structure. Neomycin has been previously shown to be able to cleave RNA in mild conditions.<sup>[18]</sup> This effect was particularly pronounced at acidic pH on HIV-1 TAR RNA. Thus, to assess whether the synthesized compounds could induce RNA cleavage on TAR RNA thanks to the presence of the conjugated moiety, we incubated increasing concentrations of compounds at 37°C at pH 7.4 (20 mM Tris·HCl, 20 mM KCl, 3 mM MgCl<sub>2</sub>). Firstly, it should be noted that histidine and imidazole alone are not able to induce any cleavage in the tested conditions. As for neomycin, it has been previously described as being able to cleave TAR RNA under acidic pH conditions<sup>[18]</sup> but under our conditions no cleavage is observed (Figure S4A in Supporting Information). Regarding the conjugated compounds (**3**, **4**, **7** and His-Napht), they all induce non-specific cleavages at high concentrations ( $> 50 \mu\text{M}$ , see Figure S4B in Supporting Information) but only compounds **3** and **4** induce a selective cleavage at lower concentrations, while **7** and His-Napht do not induce any efficient cleavage (Figure S4C in Supporting Information). Compounds **3** and **4** preferentially cleave in the single-stranded residues (U23, C24 and U25) of the bulge (Figure 2A and Figures S3 and S4 in Supporting Information) although single-stranded residues of the loop (in particular U31) are also cleaved to a lesser extent. Increasing the reaction time increases cleavage rates and the best conditions inducing the most specific cleavage were obtained after 16 hours incubation at 37°C. This cleavage is more important when pH increases suggesting that imidazole residue is indeed involved in the hydrolysis and probably cleaves with a general base catalysis mechanism (Figure 2B). Cleavage increased also in the presence of increasing concentrations of magnesium ions (Figure 2C), supporting

the hypothesis of a RNase-type reaction that would be catalyzed by divalent cations. These results illustrate that the cleavage activity does not seem to be correlated with the affinity since compound **7** ( $K_D$  of  $0.333 \pm 0.14 \mu\text{M}$ ) does not induce specific cleavage, unlike compound **4** which is a weaker ligand ( $K_D$  to  $1.38 \pm 0.17 \mu\text{M}$ ) that induces cleavage. Compound **3** appears as the best ligand and the one inducing the most efficient cleavage. We thus wondered if differences in the binding site of the compounds could account for these variations in the cleavage activity.

**Molecular mechanism of interaction.** Since the interaction site of a RNA ligand with a target sequence is an important feature that is strongly related to its biological activity and, in the context of this work, to the cleavage activity, we decided to explore the possible binding sites of the synthesized compounds on the TAR stem-loop RNA. As already demonstrated in the literature, neomycin binds to the stem residues located immediately below the three-nucleotide bulge that serves as the main binding site for Tat.<sup>[16, 19]</sup> First, we decided to measure the affinity of compounds **3**, **4** and **7** toward a mutated TAR sequence lacking the trinucleotide bulge of TAR. Indeed the region of this bulge is responsible for the interaction with Tat peptide and it is often a preferred site of interaction for TAR ligands. As illustrated in Table 1, compound **3** shows a loss of affinity of almost three times, while compounds **4** and **7** maintain the same affinity. This demonstrates that the binding of compounds **4** and **7** is probably independent from the bulge region, while residues U23, C24 and U25 are important for the interaction of compound **3** with TAR. This seems to suggest that it is possible to modify the binding site of neomycin on TAR RNA by conjugation with different groups since **3** specifically binds to the bulge region, while **4** and **7** bind to different sites or can adapt and interact with other regions if the bulge is absent.

To confirm these results, we then conducted molecular docking studies about the interaction of the synthesized compounds with TAR. AutoDock program was employed to this aim. Docking of compound **3** confirms that the preferred binding site could be around the bulge region where Tat binding occurs accordingly to what observed experimentally using the mutated sequence (Figure 3A). More specifically, compound **3** forms various hydrogen bonds and electrostatic interactions in the region going from U23 to A27 and efficiently interacts with all the bases of the bulge (Figure 3B and C). Docking studies performed with compound **4** suggest that this compound interacts preferentially at the stem-bulge junction with residues C19 to G21, U23 and C37 to C39 (Figure 4A) although an interaction with U23 residue is also present. Thus, compound **4** seems to have a slightly different binding site compared to **3** but it preserves a direct interaction with one of the three residues of the bulge. Nevertheless, the fact that the affinity of compound **4** for TAR without bulge is similar to the one with wildtype TAR suggests that the interactions with residues C19 to G21, and C37 to C39 are maintained in the absence of the bulge. Finally, compound **7** seems to bind preferentially to the stem region below the bulge going from G18 to A22 and from U38 to C41 (Figure 4B). This mode of binding in which none of the bulge residues are directly involved could explain the fact that compound **7** is able to bind mutated TAR without the bulge even better than the unmodified sequence.

Thus, together with binding data, docking suggests that all compounds can bind efficiently to TAR but at different sites of interaction. Indeed, compounds **3** and **4** seem to interact completely or partly with one or more residues of the bulge while compound **7** does not interact with the bulge. This could explain the fact that efficient cleavage on TAR sequence was only observed with compounds **3** and **4**. Thus, this cleavage would require a direct interaction of the imidazole with one of the bulge residues and that the stronger the interaction is with the bulge residues, the more efficient the cleavage will be as shown with compound **3** which is the best ligand for the bulge and induces the most pronounced cleavage.

**Inhibition of Tat/TAR interaction.** To test whether the TAR cleavage activity could increase the inhibitory potential of these compounds, we thus decided to study the ability of the synthesized compounds to inhibit Tat/TAR interaction *in vitro*, as it is well established in the literature that ligands binding around the bulge of TAR could prevent its interaction with the Tat peptide and intracellular partners, and thus inhibit TAR RNA function. To be effective inhibitors of the Tat TAR interaction in cells, ligands must display some selectivity for TAR over other nucleic acids competitors largely represented in cells. So, we first performed competition experiments in the presence of a large excess of intracellularly abundant nucleic acids, in particular in the presence of 100 eq. of tRNA and of DNA. As illustrated in Table 1, conjugates **3**, **4** and **7** show good selectivity for TAR in the presence of a large excess of tRNA and DNA, making them interesting candidates for the evaluation of Tat TAR inhibition. In contrast, this selectivity is not observed with neomycin alone and histidine  $\beta$ -naphthylamide as these compounds lose 3 to 8 times in affinity in the presence of DNA, which confirms the low selectivity of neomycin alone or intercalants for RNA versus DNA. Second, to further assess the potential of compounds **3**, **4** and **7**, as inhibitors of TAR biological function and to check whether the interaction site as well as the cleavage property allow an increase in inhibitory potential, we performed Tat/TAR inhibition experiments. To measure the ability to displace a Tat fragment from a preformed TAR/Tat complex, we employed a previously described procedure,<sup>[20]</sup> based on the use of a fluorescent Tat peptide fragment (amino acids 48–57) labeled with rhodamine and a dabcyf-labeled TAR fragment (nucleotides 18–44). In the absence of ligand, association of these two components results in an efficient quenching of the dyes by FRET. Upon addition of increasing amounts of ligands, one can observe differences in the measured  $IC_{50}$  values (Table 2 and Figure S4 in Supporting Information). As expected, the three compounds **3**, **4** and **7** can inhibit the Tat TAR interaction with  $IC_{50}$ s ranging from 0.461  $\mu$ M to 1.93  $\mu$ M. This is not surprising as it is well established in the literature that ligands interacting around the bulge of TAR could prevent an interaction with the Tat protein and cellular partners, and thus inhibit TAR RNA function. However, a closer look at the results shows that compounds **3** and **4** ( $IC_{50} \approx 0.5 \mu$ M) inhibit the Tat-TAR interaction four times better than compound **7** ( $IC_{50} \approx 2 \mu$ M), which is no more effective than neomycin alone. This suggests that the binding site of the RNA ligands on the target sequence is absolutely essential to prevent the biological functions and/or interactions of the target and compounds **3** and **4** both interacting with the bulge residues and inducing their cleavage show a very good inhibition activity compared to **7** that binds to the stem region. Among all compounds, **3** confirms

to be an excellent TAR ligand and very good inhibitor for Tat/TAR interaction *in vitro*. This is likely due to the fact that differently from compounds **4** and **7**, the three different moieties constituting compound **3**, i.e. neomycin, triazole linker and histidine, seem to be involved in the interaction with TAR RNA to bind the target in a cooperative manner.

## Conclusions

In conclusion, we designed new conjugates containing the well-known RNA ligand neomycin and imidazole-containing moieties and we performed their synthesis using a straightforward synthetic methodology allowing us to obtain desired conjugates in 2 or 3 steps starting from the previously prepared 5'-azido neomycin compound **NeoN<sub>3</sub>**. The synthesized compounds were studied on HIV-1 TAR RNA that is not only an interesting antiviral target but also an ideal model to measure the affinity and evaluate the potential biological activity of RNA ligands. Sub-micromolar affinities could be measured for compounds **3** and **7** while compound **4** maintained the same affinity as the parent compound neomycin suggesting that the presence of the amino acid histidine is important for binding. Importantly, compounds **3** and **4** showed the ability to cleave TAR RNA in physiological conditions at 37°C at the level of the bulge single-stranded residues. This property was correlated to the binding of compounds **3** and **4** that occurs with the bulge residues contrarily to compound **7** that seems to interact with the stem region as demonstrated by experiments performed on a mutated TAR sequence and by molecular docking studies. These differences in the binding sites were linked to the variation in the inhibition of Tat/TAR interactions where compounds **3** and **4** were more efficient than **7** and neomycin. Noteworthy, all synthesized compounds were selective against tRNA and DNA.

Altogether these results showed the potential of the strategy based on the straightforward preparation of RNA binders that could not only be specific for a therapeutically relevant RNA based on the chemical structure of the ligand, but also able to cleave and induce a stronger biological effect thanks to the conjugation of imidazole or histidine moieties thus opening the way to the design of more specific and efficient ligands and inhibitors. Despite the fact that the described compounds are not optimized yet, the obtained results are particularly promising for the design of conjugates containing imidazole moieties conjugated to RNA ligands specific for therapeutically relevant and complex RNA structures such as miRNAs or lncRNAs.

## Experimental Section

### Chemistry

Reagents and solvents were purchased from Aldrich, Alfa Aesar, Fluorochem, ABCR, Carlo Erba, Acros and used without further purification. Flash column chromatography was carried out on silica gel columns (Interchim Puriflash silica HP 15 to 50 µm) on Puriflash® instrument (Interchim). Analytical

thin-layer chromatography (TLC) was conducted on Sigma Aldrich precoated silica gel and compounds were visualized by irradiation (254 nm) and/or by staining with ninhydrin or vanilin stains.

$^1\text{H}$  and  $^{13}\text{C}$  NMR spectra were recorded on Bruker AC 200 and 400 MHz spectrometers. Chemical shifts are reported in parts per million (ppm,  $\delta$ ) referenced to the residual  $^1\text{H}$  resonance of the solvent ( $\text{D}_2\text{O}$   $\delta$  4.79;  $\text{CDCl}_3$   $\delta$  7.26;  $\text{CD}_3\text{OD}$   $\delta$  3.31) and referenced to the residual  $^{13}\text{C}$  resonance of the solvent ( $\text{CDCl}_3$   $\delta$  77.2;  $\text{CD}_3\text{OD}$   $\delta$  49.0). Splitting patterns are designed as follows: s (singlet), d (doublet), t (triplet), m (multiplet), and br (broad). Coupling constant (J) are listed in hertz (Hz).

Low resolution mass spectra (MS) were obtained with a Bruker Daltonics Esquire 3000+ electrospray spectrometer equipped with API ionization source. High-resolution mass spectrometry (HRMS) was carried out on a LTQ Orbitrap hybrid mass spectrometer with an electrospray ionization probe (ThermoScientific, San Jose, CA) by direct infusion from a pump syringe, to confirm the correct molar mass and high purity of the compounds.

HPLC analyses were performed using a Water Alliance 2695 pump coupled to a Water 996 photodiode array detector and a X-Select CSH<sup>TM</sup> fluorophenyl reverse-phase C18 column (50 x 4.6 mm, 5  $\mu\text{m}$ ) for analytical HPLC analysis. All experiments were run out at room temperature using a gradient of  $\text{CH}_3\text{CN}$  containing 0.1% TFA (eluent B) in water containing 0.1% TFA (eluent A) from 5% to 100% of eluent B over 30 min at flow rates of 0.9 mL/min for analytical HPLC.

## Synthetic procedures

### General procedures

#### General procedure A – Huisgen 1,3-dipolar cycloaddition with copper

To a solution of  $(\text{Boc})_6$ -neomycin- $\text{N}_3$  (30 mg, 0.0240 mmol) prepared as previously described<sup>[12e]</sup> in 1 mL of  $\text{CH}_3\text{CN}$  were added alkynes **8** or **10** (1.3 eq.),  $\text{CuI}$  (3.7 mg, 0.0194 mmol, 0.8 eq) and *N,N*-diisopropylethylamine (25  $\mu\text{L}$ , 0.144 mmol, 6 eq). The reaction mixture was stirred overnight at room temperature, then the solvent was removed under reduced pressure. Water was added and the mixture was extracted with  $\text{CH}_2\text{Cl}_2$ . The combined organic phases were washed with EDTA (50 eq.) and brine, dried over  $\text{Na}_2\text{SO}_4$  and then concentrated under reduced pressure. The crude residue was purified by flash chromatography on a silica gel column using a mixture  $\text{CH}_2\text{Cl}_2/\text{MeOH}$  97:3 as the eluent to provide the desired compounds **1** and **3**.

#### General procedure B - Boc deprotection with TFA

To a solution of Boc-protected-products **1**, **3** or **6** in  $\text{CH}_2\text{Cl}_2$  was added TFA (50 eq.) and the reaction mixture was stirred 4 h at room temperature. Solvent was removed under reduced pressure and the residual TFA co-evaporated with toluene. The product was precipitated in  $\text{Et}_2\text{O}$  and lyophilized to give the desired products **2**, **4** and **7**.

**(Boc)<sub>6</sub>-Neomycin-5''-[N-Boc-L-His(Boc)-acetamido]triazole (1)**. Compound **1** was prepared following general procedure A and obtained as a white solid in 96% yield (33.5 mg).  $R_f$  = 0.30 ( $\text{CH}_2\text{Cl}_2/\text{MeOH}$  95:5);  $^1\text{H}$  NMR (400 MHz,  $\text{CD}_3\text{OD}$ )  $\delta$  8.11 (s, 1H), 8.03 (s, 1H), 7.26 (s, 1H), 5.42 (s,

1H), 5.11 (s, 1H), 4.95 (s, 1H), 4.75 – 4.70 (m, 1H), 4.70-4.65 (m, 1H), 4.60-4.55 (m, 1H), 4.50-4.40 (m, 1H), 4.40-4.30 (m, 3H), 4.20-4.10 (m, 1H), 4.00-3.95 (m, 1H), 3.95-3.90 (m, 1H), 3.80-7.75 (m, 2H), 3.70 – 3.50 (m, 4H), 3.50-3.40 (m, 5H), 3.30-3.25 (m, 1H), 3.25-3.20 (m, 1H), 3.20-3.10 (m, 1H), 3.95-2.85 (m, 1H), 2.00 – 1.90 (m, 1H), 1.63 (s, 9H), 1.55 – 1.30 (m, 64H); <sup>13</sup>C NMR (101 MHz, CD<sub>3</sub>OD) δ 173.8, 159.2, 158.9, 158.5, 158.2, 158.1, 157.9, 157.5, 148.1, 145.4, 140.1, 138.3, 126.3, 116.3, 111.5, 100.4, 98.9, 87.1, 86.2, 80.7, 80.4, 80.2, 79.9, 75.4, 74.6, 74.4, 73.0, 72.9, 72.8, 71.6, 69.0, 56.6, 55.5, 53.6, 53.1, 52.6, 51.1, 42.4, 42.0, 35.9, 35.9, 31.9, 28.9, 28.8, 28.8, 28.1; MS (ESI) *m/z* 1632.33 (M+H)<sup>+</sup> (C<sub>72</sub>H<sub>121</sub>N<sub>13</sub>O<sub>29</sub> requires 1632.85).

**(Boc)<sub>6</sub>-Neomycin-5''-[N-Boc-imidazole-3-propanamide]triazole (2).** Compound **2** was prepared following general procedure A and obtained as a white solid in 63% yield (22.7 mg). *R<sub>f</sub>* = 0.27 (CH<sub>2</sub>Cl<sub>2</sub>/MeOH 95:5); <sup>1</sup>H NMR (400 MHz, CD<sub>3</sub>OD) δ 8.13 (br s, 1H), 8.05 (s, 1H), 7.46 (br s, 1H), 5.42 (s, 1H), 5.12 (s, 1H), 4.96 (s, 1H), 4.70-4.50 (m, 3H), 4.40-4.30 (m, 2H), 4.25-4.15 (m, 1H), 4.00-3.90 (m, 2H), 3.80-3.70 (m, 2H), 3.70-3.35 (m, 12H), 3.30-3.25 (m, 1H), 3.20-3.10 (m, 1H), 2.00-1.90 (m, 1H), 1.64 (s, 9H), 1.60-1.40 (m, 55H); <sup>13</sup>C NMR (101 MHz, CD<sub>3</sub>OD) δ 172.2, 159.2, 158.9, 158.5, 158.2, 158.1, 158.0, 157.9, 145.5, 126.1, 111.6, 100.4, 98.9, 87.2, 86.1, 80.7, 80.4, 80.3, 79.9, 75.4, 74.5, 74.5, 73.2, 72.9, 72.8, 71.6, 69.0, 56.6, 53.6, 53.5, 52.5, 51.1, 42.4, 42.0, 36.1, 35.9, 30.8, 28.9, 28.9, 28.8, 28.8, 28.1; MS (ESI) *m/z* 752.00 [(M+2H)/2]<sup>2+</sup> (C<sub>66</sub>H<sub>111</sub>N<sub>12</sub>O<sub>27</sub> requires 1503.77).

**Neomycin-5''-[L-His-acetamido]triazole (3).** Compound **2** was prepared following general procedure B starting from compound **1** (31.9 mg, 0.0200 mmol) in the presence of TFA (50 μL) in CH<sub>2</sub>Cl<sub>2</sub> (1 mL). Compound **2** was obtained as a white solid (26.5 mg, 78%). Retention time 1.8 min; <sup>1</sup>H NMR (400 MHz, D<sub>2</sub>O) δ 8.69 (s, 1H), 8.04 (s, 1H), 7.37 (s, 1H), 6.05 (d, *J* = 3.7 Hz, 1H), 5.43 (d, *J* = 2.4 Hz, 1H), 5.32 (s, 1H), 4.55-4.45 (m, 4H), 4.35-4.25 (m, 3H), 4.15 – 4.05 (m, 1H), 4.05 – 3.90 (m, 4H), 3.85 (br s, 1H), 3.70 (t, *J* = 9.8 Hz, 1H), 3.65 – 3.50 (m, 4H), 3.50 – 3.31 (m, 8H), 2.55-2.45 (m, 1H), 2.00-1.90 (m, 1H); <sup>13</sup>C NMR (101 MHz, D<sub>2</sub>O) δ 167.9, 144.0, 134.4, 125.8, 124.6, 120.7, 118.3, 117.8, 114.9, 110.2, 95.5, 95.0, 85.0, 79.7, 75.0, 72.9, 72.4, 70.5, 70.2, 69.7, 67.6, 67.4, 53.3, 52.1, 50.8, 49.6, 48.4, 40.4, 40.0, 34.3, 27.9, 26.0; HRMS (ESI) *m/z* 832.42743 (M+H)<sup>+</sup> (C<sub>32</sub>H<sub>58</sub>N<sub>13</sub>O<sub>13</sub> requires 832.42716).

**Neomycin-5''-[imidazole-3-propanamide]triazole (4).** Compound **4** was prepared following general procedure B starting from compound **2** (32.6 mg, 0.0220 mmol), and TFA (50 μL) in CH<sub>2</sub>Cl<sub>2</sub> (1 mL). The product was precipitated in Et<sub>2</sub>O leading to compound **4** as a white solid in 76% yield (26.7 mg). Retention time 2.0 min; <sup>1</sup>H NMR (400 MHz, D<sub>2</sub>O) δ 8.65 (s, 1H), 8.01 (s, 1H), 7.34 (s, 1H), 6.03 (d, *J* = 3.8 Hz, 1H), 5.41 (d, *J* = 3.3 Hz, 1H), 5.31 (d, *J* = 1.1 Hz, 1H), 4.60-4.55 (m, 1H), 4.55-4.50 (m, 2H), 4.44 (t, *J* = 5.1 Hz, 1H), 4.32 (t, *J* = 4.4 Hz, 1H), 4.27-4.19 (m, 1H), 4.20-4.00 (m, 2H), 4.00-3.90 (m, 3H), 3.90-3.80 (m, 3H), 3.75-3.65 (m, 1H), 3.65-3.50 (m, 4H), 3.50-3.30 (m, 5H), 2.55-2.45 (m, 1H), 1.90-1.80 (m, 1H); <sup>13</sup>C NMR (101 MHz, D<sub>2</sub>O) δ 170.5, 133.6, 126.5, 124.5, 117.5, 110.1, 95.6, 95.0, 85.0, 76.8, 75.0, 72.95, 72.9, 72.4, 70.4, 70.2, 69.7, 68.0, 67.6, 67.4, 53.2, 51.9, 50.8, 49.6, 48.4, 40.4, 40.0, 34.6, 30.8, 27.9; HRMS (ESI) *m/z* 803.40070 (M+H)<sup>+</sup> (C<sub>31</sub>H<sub>55</sub>N<sub>12</sub>O<sub>13</sub> requires 803.40061).

**(Boc)<sub>6</sub>-Neomycin-5''-[N-Boc-L-His(Boc)]-amide (6).** To a solution of *N*α,*N*im-di-Boc-L-histidine (16.1 mg, 0.0299 mmol) in 1.5 mL of a mixture CH<sub>2</sub>Cl<sub>2</sub> /DMF 1:1 were added EDC (9.75 mg, 0.0409 mmol, 1.7 eq.) and HOSu (5.86 mg, 0.0409 mmol, 1.7 eq.). The reaction mixture was stirred at room temperature for 2h before adding the amino derivative of neomycin **5** (40 mg, 0.0329 mmol, 1.3 eq.) prepared following a previously reported procedure.<sup>[21]</sup> The reaction mixture was stirred overnight at room temperature. Water was added and the mixture was extracted with CH<sub>2</sub>Cl<sub>2</sub>. The combined organic phases were washed with water and brine, dried over Na<sub>2</sub>SO<sub>4</sub> and then concentrated under reduced pressure. The crude residue was purified by flash chromatography on a silica gel column using a mixture CH<sub>2</sub>Cl<sub>2</sub>/MeOH 95:5 as the eluent to provide desired compound **6** as a white solid in 71% yield (32.5 mg). *R<sub>f</sub>* = 0.46 (CH<sub>2</sub>Cl<sub>2</sub>/MeOH 95:5); <sup>1</sup>H NMR (400 MHz, CD<sub>3</sub>OD) δ 8.16 (s, 1H), 7.33 (s, 1H), 6.68 (br s, 1H), 5.40-5.30 (m, 1H), 5.20-5.10 (m, 1H), 4.50-4.40 (m, 1H), 4.30-4.25 (m, 1H), 4.20-4.00 (m, 2H), 3.70-3.40 (m, 10H), 3.20-3.10 (m, 1H), 2.90-2.80 (m, 1H), 2.00-1.90 (m, 1H), 1.63 (s, 9H), 1.50-1.25 (m, 64H); HRMS (ESI) *m/z* 1451.76294 (M+H)<sup>+</sup> (C<sub>64</sub>H<sub>111</sub>N<sub>10</sub>O<sub>27</sub> requires 1451.76146).

**Neomycin-5''-L-His-amide (7).** Compound **7** was prepared following general procedure B starting from compound **6** (29.0 mg, 0.019 mmol), and TFA (100 μL) in CH<sub>2</sub>Cl<sub>2</sub> (1 mL). The product was precipitated in Et<sub>2</sub>O leading to compound **6** as a white solid in 59% yield (18.6 mg). Retention time min 1.7 min; <sup>1</sup>H NMR (400 MHz, D<sub>2</sub>O) δ 8.70 (s, 1H), 7.43 (s, 1H), 5.93 (d, *J* = 3.0 Hz, 1H), 5.40 (d, *J* = 2.9 Hz, 1H), 5.30 (s, 1H), 4.40 – 4.30 (m, 3H), 4.25-4.20 (m, 2H), 4.20-4.15 (m, 1H), 4.11 (t, *J* = 9.7 Hz, 1H), 4.10-3.95 (m, 3H), 3.85-3.80 (m, 1H), 3.80 – 3.65 (m, 3H), 3.65-3.60 (m, 1H), 3.60-3.50 (m, 2H), 3.50 – 3.25 (m, 8H), 2.55-2.50 (m, 1H), 1.91 (q, *J* = 12.6 Hz, 1H); <sup>13</sup>C NMR (101 MHz, D<sub>2</sub>O) δ 168.8, 134.6, 118.3, 117.8, 114.9, 109.1, 95.7, 95.3, 84.7, 80.9, 76.8, 75.3, 73.0, 72.3, 70.5, 70.0, 69.7, 68.1, 67.5, 53.2, 52.1, 50.8, 49.6, 48.5, 41.8, 40.5, 40.1, 27.9, 26.3; HRMS (ESI) *m/z* 751.39447 (M+H)<sup>+</sup> (C<sub>29</sub>H<sub>55</sub>N<sub>10</sub>O<sub>13</sub> requires 751.39446).

## Acknowledgments

Thanks are due to J. M. Guigonis (Plateforme Bernard Rossi, CEA TIRO, Nice, France) for HRMS analyses and to S. Kovachka for her help in preparing docking illustrations. PhD fellowship (to C.M.) is supported by grant from Agence Nationale de la Recherche (ANR-17-CE18-0009). PhD fellowship (to M.B.) is supported by French Minister for Research and Higher Education.

## Keywords

inhibition, medicinal chemistry, neomycin, RNA cleavage, RNA targeting

## Figures

**Figure 1.** A) General structure of the imidazole-neomycin conjugates synthesized in this study. B) Primary and secondary structure of 59-mer HIV-1 TAR RNA in interaction with its intracellular partners Tat, Cyclin T1 and CDK9.

**Figure 2.** PAGE analysis of Alexa488<sup>TM</sup> end-labelled TAR RNA after incubation with compound **3** showing three major cleavage products (highlighted in the black square). Conditions: 1 mM 5'-Alexa<sup>488</sup>-TAR, 20 mM Tris·HCl (pH 7.4), 1 mM EDTA, 5 mM MgCl<sub>2</sub>, 12 mM NaCl, 16 h reaction time at 37°C in the presence of A) increasing concentrations of compound **3** (0.1 μM in lane 4, 0.5 μM in lane 5, 1 μM in lane 6, 5 μM in lane 7, 10 μM in lane 8 and 50 μM in lane 9); B) compound **3** at 10 μM in the presence of increasing pH (6.5 in lane 4, 7 in lane 5, 7.5 in lane 6, 8 in lane 7 and 8.5 in lane 8); C) compound **3** at 10 μM in the presence of increasing concentrations of MgCl<sub>2</sub> (0 mM in lane 4, 3 mM in lane 5, 5 mM in lane 6 and 10 mM in lane 7). For all gels, lane 1: RNA only, lane 2 alkaline hydrolysis ladder; lane 3: T1 treatment (15 minutes at 37°C); D) Primary and secondary structure of 27-mer TAR RNA where the binding site of compound **3** is indicated by orange circles and the main cleavage sites by arrows.

**Figure 3.** A) Primary and secondary structure of 27-mer TAR RNA employed during this study. Orange circles indicate the binding site of compound **3**. B) Docking of **3** with the TAR RNA hairpin loop performed by using Autodock in which the grid boxes were fixed on the entire RNA sequence. C) Focus on the binding pocket of the docking results for the interaction of **3** with TAR RNA. D) Chemical structure of compound **3** where the main interactions between the compound and the RNA residues are indicated by arrows.

**Figure 4.** A) Primary and secondary structure of 27-mer TAR RNA employed during this study. Orange circles indicate the binding site of compound **4** and chemical structure of compound **4** where the main interactions between the compound and the RNA residues are indicated by arrows. B) Docking of **4** with the TAR RNA hairpin loop performed by using autodock in which the grid boxes were fixed on the entire RNA sequence. C) Primary and secondary structure of 27-mer TAR RNA employed during this study. Orange circles indicate the binding site of compound **7** and chemical structure of compound **7** where the main interactions between the compound and the RNA residues are indicated by arrows. D) Docking of **7** with the TAR RNA hairpin loop performed by using autodock in which the grid boxes were fixed on the entire RNA sequence.

**Scheme 1.** Synthesis of neomycin conjugates **3**, **4** and **7**. Reagents: a) *N*-Boc-L-His(Boc)-propargylamide (for compound **1**) and *N*-2-Propyn-1-yl-1*H*-imidazole-5-propanamide (for compound **2**), CuI, DIPEA, CH<sub>3</sub>CN, overnight, r.t.; b) TFA, CH<sub>2</sub>Cl<sub>2</sub>, 4h, r.t.; c) H<sub>2</sub>, Pd/C, EtOH, 4h, r.t.; d) HOSu, EDC, CH<sub>2</sub>Cl<sub>2</sub>/DMF 1:1, r.t. overnight.



Figure 2.

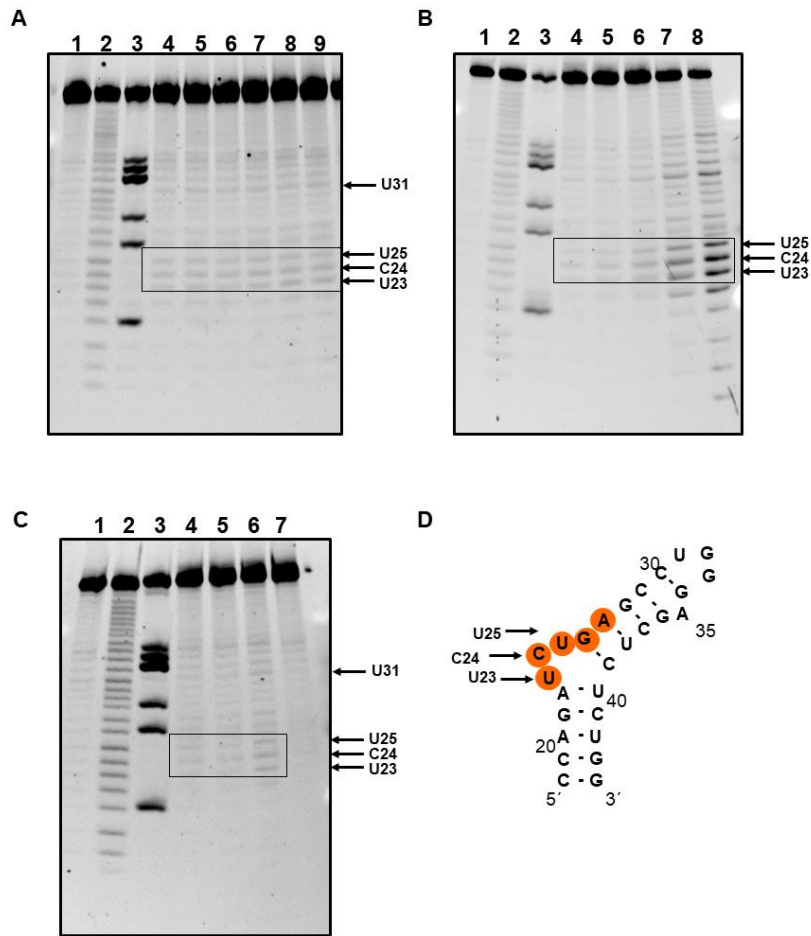


**Figure 3.**

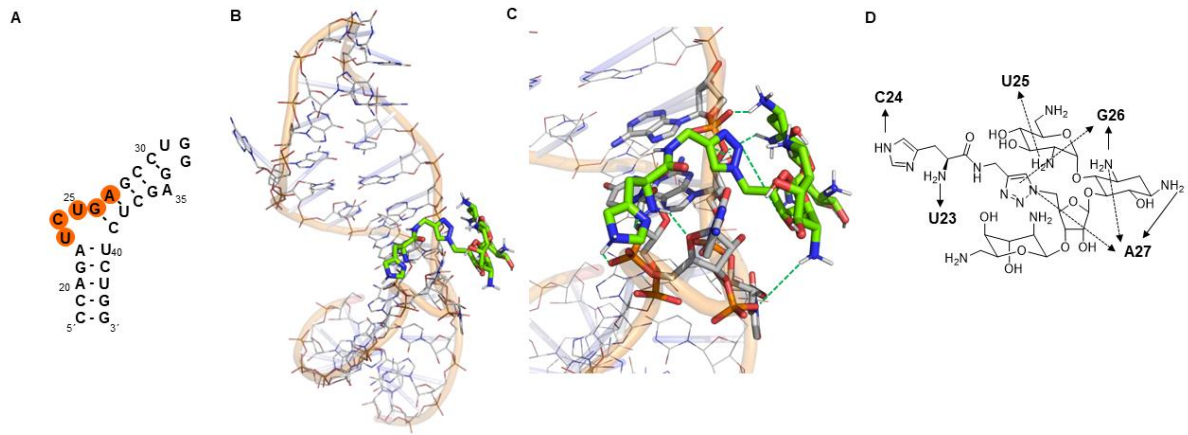
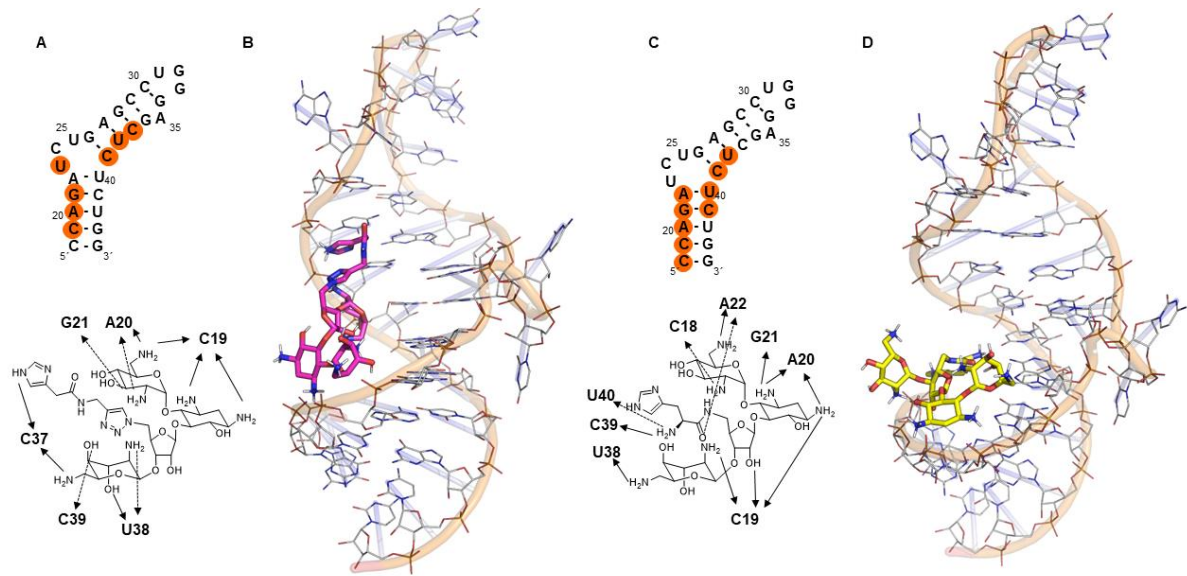
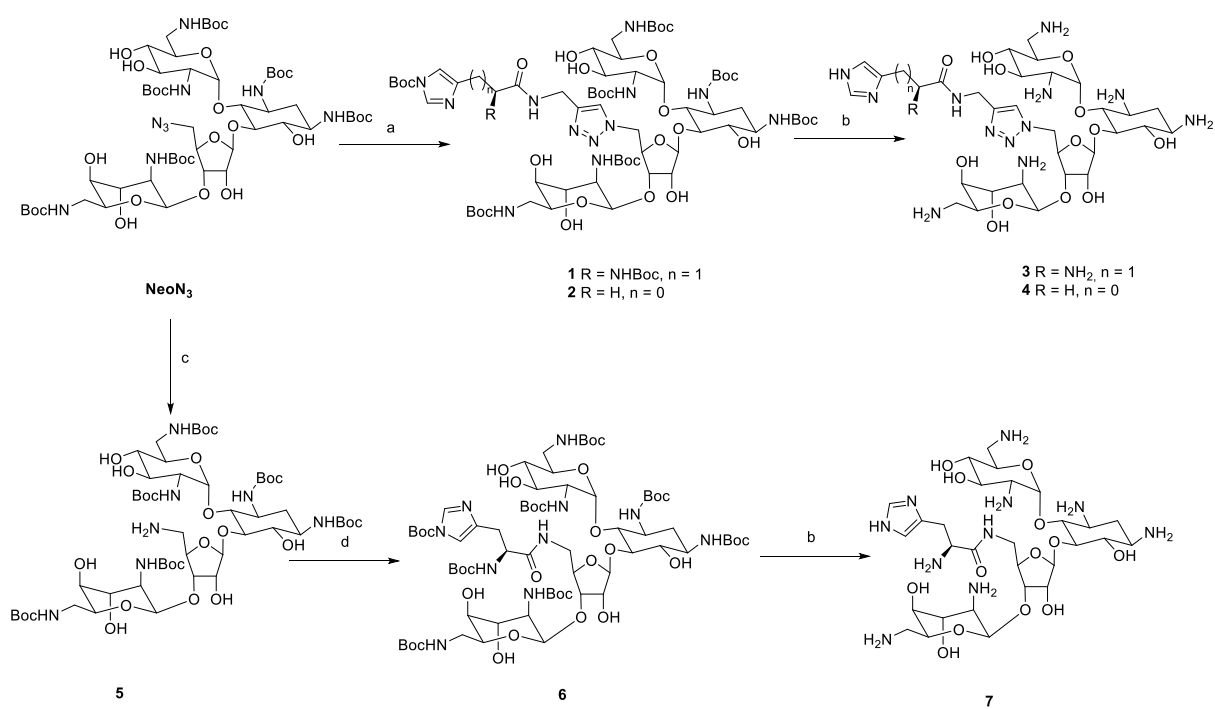


Figure 4.



### Scheme 1.



**Table 1.** Dissociation constants ( $K_D$ ) measured on a 27-mer 5'-Alexa<sup>488</sup> TAR RNA sequence as well as in the presence of a 24-mer 5'-Alexa<sup>488</sup> TAR RNA lacking the three residues of the bulge. Competition experiments were performed in the presence of 100 eq. of tRNA ( $K'_D$ ) and DNA ( $K''_D$ ). All values are expressed in  $\mu\text{M}$ .

ID	$K_D^a$	$K_D$ (TAR without bulge) <sup>a</sup>	$K'_D$ (tRNA) <sup>b</sup>	$K'_D/K_D$	$K''_D$ (DNA) <sup>b</sup>	$K''_D/K_D$
<b>Neomycin</b>	$1.74 \pm 0.16$	-	$8.70 \pm 0.22$	5.0	$5.47 \pm 1.7$	3.4
<b>3</b>	$0.0838 \pm 0.0015$	$0.239 \pm 0.022$	$0.116 \pm 0.029$	1.4	$0.144 \pm 0.042$	1.7
<b>4</b>	$1.38 \pm 0.17$	$1.41 \pm 0.19$	$1.94 \pm 0.26$	1.4	$1.83 \pm 0.37$	1.3
<b>7</b>	$0.333 \pm 0.14$	$0.216 \pm 0.019$	$0.430 \pm 0.11$	1.3	$0.567 \pm 0.24$	1.7
<b>Histidine</b>	no binding	-	-	-	-	-
<b>Imidazole</b>	no binding	-	-	-	-	-
<b>His-Naphth</b>	$13.6 \pm 4.4$	$18.4 \pm 8.0$	$26.1 \pm 5.1$	1.9	$106 \pm 10$	7.8

<sup>a</sup> Binding studies were performed on 5'-Alexa<sup>488</sup>-TAR RNA and mutated 5'-Alexa<sup>488</sup>-TAR RNA lacking the bulge residues in buffer A (20 mM Tris-HCl (pH 7.4), 12 mM NaCl, 2.5 mM MgCl<sub>2</sub> and 1 mM DTT). <sup>b</sup> Competitions experiments were performed in the presence of a 100-equivalent excess of tRNA ( $K'_D$ ) or DNA ( $K''_D$ ).

**Table 2.** IC<sub>50</sub> values (μM) for the inhibition of Tat/TAR interaction. 5'-dabcyl-TAR 27-mer and Tat48–57 peptide (sequence: Rhodamine-YGRKKRRQRRRP, EzBiolab, USA) were both used at concentrations of 10 nM in buffer B (50 mM Tris–HCl, 20 mM KCl, 0.02% Tween 20, pH 7.4).

<b>ID</b>	<b>IC<sub>50</sub> (μM)</b>
<b>Neomycin</b>	1.26 ± 0.23
<b>3</b>	0.683 ± 0.10
<b>4</b>	0.461 ± 0.050
<b>7</b>	1.93 ± 0.77
<b>His-Naphth</b>	> 500 μM

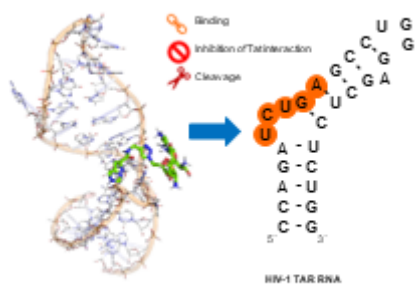
## References

- [1] J. P. Falese, A. Donlic, A. E. Hargrove, *Chem. Soc. Rev.* **2021**, *50*, 2224-2243.
- [2] K. D. Warner, C. E. Hajdin, K. M. Weeks, *Nat. Rev. Drug Discov.* **2018**, *17*, 547-558.
- [3] S. T. Crooke, B. F. Baker, R. M. Crooke, X. H. Liang, *Nat. Rev. Drug Discov.* **2021**, *20*, 427-453.
- [4] S. M. Meyer, C. C. Williams, Y. Akahori, T. Tanaka, H. Aikawa, Y. Tong, J. L. Childs-Disney M. D. Disney, *Chem. Soc. Rev.* **2020**, *49*, 7167-7199.
- [5] D. N. Wilson, *Nat. Rev. Microbiol.* **2014**, *12*, 35-48.
- [6] H. Ratni, M. Ebeling, J. Baird, S. Bendels, J. Bylund, K. S. Chen, N. Denk, Z. Feng, L. Green, M. Guerard, P. Jablonski, B. Jacobsen, O. Khwaja, H. Kletzl, C. P. Ko, S. Kustermann, A. Marquet, F. Metzger, B. Mueller, N. A. Naryshkin, S. V. Paushkin, E. Pinard, A. Poirier, M. Reutlinger, M. Weetall, A. Zeller, X. Zhao, L. Mueller, *J. Med. Chem.* **2018**, *61*, 6501-6517.
- [7] M. D. Disney, A. M. Winkelsas, S. P. Velagapudi, M. Southern, M. Fallahi, J. L. Childs-Disney, *ACS Chem. Biol.* **2016**, *11*, 1720-1728.
- [8] a) L. Guan, M. D. Disney, *Angew. Chem. Int. Ed. Engl.* **2013**, *52*, 1462-1465; b) N. Tamkovich, L. Koroleva, M. Kovpak, E. Goncharova, V. Silnikov, V. Vlassov, M. Zenkova, *Bioorg. Med. Chem.* **2016**, *24*, 1346-1355.
- [9] a) J. D. Ballin, J. P. Prevas, C. R. Ross, E. A. Toth, G. M. Wilson, M. T. Record, Jr., *Biochemistry* **2010**, *49*, 2018-2030; b) S. Fouace, C. Gaudin, S. Picard, S. Corvaisier, J. Renault, B. Carboni, B. Felden, *Nucleic Acids Res.* **2004**, *32*, 151-157; c) C. Gamble, M. Trotard, J. Le Seyec, V. Abreu-Guerniou, N. Gernigon, F. Berree, B. Carboni, B. Felden, R. Gillet, *Bioorg. Med. Chem. Lett.* **2009**, *19*, 3581-3585.
- [10] a) A. J. Angelbello, M. D. Disney, *ChemBioChem* **2018**, *19*, 43-47; b) A. J. Angelbello, S. G. Rzuczek, K. K. McKee, J. L. Chen, H. Olafson, M. D. Cameron, W. N. Moss, E. T. Wang, M. D. Disney, *Proc. Natl. Acad. Sci. U S A* **2019**, *116*, 7799-7804.
- [11] H. S. Haniff, Y. Tong, X. Liu, J. L. Chen, B. M. Suresh, R. J. Andrews, J. M. Peterson, C. A. O'Leary, R. I. Benhamou, W. N. Moss, M. D. Disney, *ACS Cent. Sci.* **2020**, *6*, 1713-1721.
- [12] a) J. P. Joly, M. Gaysinski, L. Zara, M. Duca, R. Benhida, *Chem. Commun. (Camb)* **2019**, *55*, 10432-10435; b) J. P. Joly, G. Mata, P. Eldin, L. Briant, F. Fontaine-Vive, M. Duca, R. Benhida, *Chem. Eur. J.* **2014**, *20*, 2071-2079; c) C. Maucort, D. D. Vo, S. Aouad, C. Charrat, S. Azoulay, A. Di Giorgio, M. Duca, *ACS Med Chem Lett* **2021**, *12*, 899-906; d) D. D. Vo, C. Becquart, T. P. A. Tran, A. Di Giorgio, F. Darfeuille, C. Staedel, M. Duca, *Org. Biomol. Chem.* **2018**, *16*, 6262-6274; e) D. D. Vo, C. Staedel, L. Zehnacker, R. Benhida, F. Darfeuille, M. Duca, *ACS Chem. Biol.* **2014**, *9*, 711-721; f) D. D. Vo, T. P. Tran, C. Staedel, R. Benhida, F. Darfeuille, A. Di Giorgio, M. Duca, *Chem. Eur. J.* **2016**, *22*, 5350-5362.
- [13] K. Aradi, A. Di Giorgio, M. Duca, *Chem. Eur. J.* **2020**, *26*, 12273-12309.

- [14] a) C. Martin, S. D. Piccoli, M. Gaysinski, C. Becquart, S. Azoulay, A. D. Giorgio, M. Duca, *ChemPlusChem* **2020**, *85*, 207-216; b) C. Staedel, T. P. A. Tran, J. Giraud, F. Darfeuille, A. Di Giorgio, N. J. Tourasse, F. Salin, P. Uriac, M. Duca, *Sci. Rep.* **2018**, *8*, 1667.
- [15] J. R. Thomas, P. J. Hergenrother, *Chem. Rev.* **2008**, *108*, 1171-1224.
- [16] S. Wang, P. W. Huber, M. Cui, A. W. Czarnik, H. Y. Mei, *Biochemistry* **1998**, *37*, 5549-5557.
- [17] T. P. A. Tran, S. Poulet, M. Pernak, A. Rayar, S. Azoulay, A. D. Giorgio, M. Duca, *RSC Med. Chem.* **2022**, 311-319.
- [18] M. J. Belousoff, B. Graham, L. Spiccia, Y. Tor, *Org. Biomol. Chem.* **2009**, *7*, 30-33.
- [19] C. Faber, H. Sticht, K. Schweimer, P. Rosch, *J. Biol. Chem.* **2000**, *275*, 20660-20666.
- [20] A. I. Murchie, B. Davis, C. Isel, M. Afshar, M. J. Drysdale, J. Bower, A. J. Potter, I. D. Starkey, T. M. Swarbrick, S. Mirza, C. D. Prescott, P. Vaglio, F. Aboul-ela, J. Karn, *J. Mol. Biol.* **2004**, *336*, 625-638.
- [21] L. Jiang, D. Watkins, Y. Jin, C. Gong, A. King, A. Z. Washington, K. D. Green, S. Garneau-Tsodikova, A. K. Oyelere, D. P. Arya, *ACS Chem. Biol.* **2015**, *10*, 1278-1289.

## Table of Contents

**New RNA binders:** a straightforward synthetic methodology allowed to obtain new neomycin conjugates containing an imidazole residue mimicking the active site of ribonuclease enzymes able to induce a site-specific cleavage of HIV-1 TAR RNA in physiological conditions. We found compounds with excellent affinity, promising cleavage activity and the ability to inhibit Tat/TAR interaction with submicromolar  $IC_{50}$ s.



Twitter handles are @MariaDuca\_CNRS @INC\_CNRS and @NiceChemistry